LA-UR-80-2921

CONF-801011--49

TITLE: A COMPACT-TOROID FUSION REACTOR BASED ON THE FIELD-REVERSED THETA-PINCH REACTOR SCALING AND OPTIMIZATION FOR CTOR

AUTHOR(S): R. L. Hagenson and R. A. Krakowski

SUBMITTED TO: 4th ANS Topical Meeting on the Technology of Controlled Nuclear Fusion
King of Prussia, PA (October 14-17, 1980)

MASTER

University of California

LOS ALAMOS SCIENTIFIC LABORATORY
Post Office Box 1663 Los Alamos, New Mexico 87545
An Affirmative Action/Equal Opportunity Employer

Form No. 836 R3
St. No. 2629

UNITED STATES
DEPARTMENT OF ENERGY

A COMPACT-TOROID FUSION REACTOR BASED ON THE FIELD-REVERSED THETA PINCH: REACTOR SCALING AND OPTIMIZATION FOR CTOR*

R. L. Hagenson** and R. A. Krakowski
Los Alamos Scientific Laboratory
Los Alamos, NM 87545

ABSTRACT

Early scoping studies based on approximate, analytic models have been extended on the basis of a dynamic plasma model and an overall systems approach to examine a Compact Toroid (CT) reactor embodiment that uses a Field-Reversed Theta Pinch as a plasma source. The field-reversed plasmoid would be formed and compressionally heated to ignition prior to injection into and translation through a linear burn chamber, thereby removing the high-technology plasmoid source from the hostile reactor environment. Stabilization of the field-reversed plasmoid would be provided by a passive conduction shell located outside the high-temperature blanket but within the low-field superconducting magnets and associated radiation shielding. On the basis of this batch-burn but thermally steady-state approach a reactor concept emerges with a length below ~ 40 m that generates 300-400 MWe of net electrical power with a recirculating power fraction less than 0.15.

I. INTRODUCTION

A Compact Toroid (CT) is a plasma configuration in which no magnetic coils or structural walls extend through the torus. Although conceptually not a new idea[1], interest in this configuration was re-kindled with the proposal of the spheromak reactor.[2,3] The level of interest in CT reactors is reflected by a comprehensive, international workshop[3] on that topic and the large number of conceptual reactors that have been proposed and/or designed around the CT configuration: Field-Reversed Mirror (FRM);[4] the moving-ring FRM;[5A] the moving-ring Spheromak;[6] the Slowly-Imploding liner (Linus);[7] the Trigger-Reconnected Adiabatically-Compressed Torus (TRACT);[8] Antron-like ion-ring devices;[9] and the Field-Reversed Theta-Pinch (FRTP) reactor (CTOR).[10] In one instance even the Reversed-Field Pinch (RFP)[11] has been claimed[6] as a member of the CT family. Generally, plasmoids without toroidal field are classified[10] as Field-Reversed Configurations (FRC), whereas systems containing toroidal fields are termed spheromaks. An FRC or spheromak plasmoid in a reactor embodiment may translate[5,6,9,10] through or be held stationary[2,3,4,7,8] in a linear burn chamber. These 9-10 CT reactor proposals have one common feature; although a computational understanding of equilibrium/stability requirements is rapidly developing, little is known quantitatively for use in reactor prognoses, and even less is known about particle/energy transport. Consequently, reactor equilibrium/stability constraints are assumed to be provided by either a passively conducting shell, an active feedback system, or finite-Larmor-radius effects; or this issue is ignored. Transport losses are generally assumed to scale according to tokamak experimental results (~ 100-200 "Bohm" times,[10] or Alcator scaling). Depending on the degree of assumption applied to the equilibrium/stability constraint, a given CT reactor may be stationary or translating, and a means to produce and sustain a stationary, steady-state plasmoid may or may not be specified. This apparent degree of arbitrariness, which legitimately characterizes a new and rapidly developing concept, makes the drawing of specific comparative conclusions risky at this time before a more comprehensive experimental or theoretical picture has been developed.

The approach taken by the LASL CT reactor study utilizes as much as possible that which is rather than that which might be. Specifically, a FRTP is selected to form a FRC (i.e., no toroidal field); adiabatic compression of the ~ 1-keV FRC to ignition is invoked; the heated and ignited FRC would be stabilized by a passive shell that assures the required ratio of separatrix-to-conductor radius. The CTOR design reported herein is batch burn and reflects as much as is possible this "design-to-state-of-art" philosophy. The major assumptions made in arriving at this CTOR design are: equilibrium constraints are given by observations made on relatively small experiments; stabilization by a passive conducting shell is possible within shell-to-plasmoid radius constraints also given by relatively small experiments; energy confinement times are given by scaling laws

*Work performed under the auspices of the U.S. Department of Energy.
**Science Applications Inc., Ames, Iowa

obtained from tokamak experiments (i.e., Alcator or 200 Bohm); nearly constant particle inventories are assumed during the burn period (i.e., few seconds), implying that the particle confinement times, τ_p, much longer than energy confinement times, τ_E, or considerable ingestion of neutral density if $\tau_p \approx \tau_E$. Lastly, active feedback of either gross or local MHD is not invoked by the CTOR design reported herein; active feedback systems placed within the reactor environment is considered unattractive compared to stabilization by a passive, exo-blanket shell, and present understanding of CT equilibrium/-stability is not sufficiently developed at this time to permit a quantitative analysis of the physics/technology requirements of an in-blanket active feedback system.

II. SUMMARY

Within the constraints imposed by these physical assumptions the CTOR as presently envisaged would use a Field-Reversed Theta Pinch (FRTP) to produce external to the reactor an FRC plasmoid that is subsequently heated and translated through a linear burn chamber. The high-voltage plasmoid source and compressional heater are removed from the burn chamber to a less hostile environment. The stabilizing conducting shell would be positioned between the blanket and shield. Translation of the ignited plasmoid, shown schematically on Fig. 1, allows portions of the conducting shell that have not experienced flux diffusion to be continually "exposed". A nearly (thermal) steady-state operation of the first wall and blanket is possible for appropriate plasmoid speeds and injection rates. Locating the stabilizing conducting shell outside the blanket permits

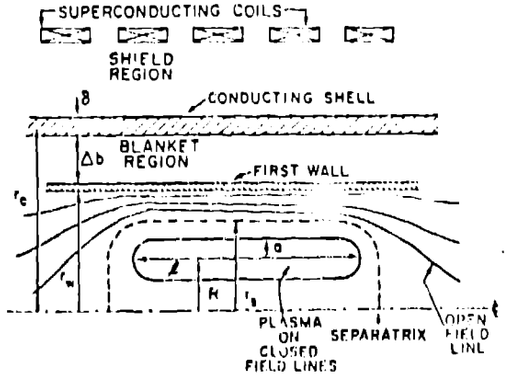

Fig. 1. Compact torus geometry showing radius of conducting shell, r_c, first wall, r_w, separatrix, r_s and plasmoid length, ℓ. This FRC plasmoid would be stabilized by a passively conducting shell of current radius r_c, and thickness δ that is located outside a breeding blanket of thickness $\Delta b \approx 0.5$ m.

room-temperature operation and minimizes the translational power, which appears as joule losses in the exo-blanket shell; these losses can be supplied directly by alpha-particle heating through modest radial expansion of the plasmoid inside a slightly flared conducting shell, blanket and first wall. Translational runaway is prevented by the presence of a thin (~ 1-mm) first-wall "shell" that is highly permeable to magnetic flux penetration but which nevertheless stabilizes the linear motion. Superconducting coils are located outside the blanket, conducting shell and shield to provide a continuous bias field that is compressed between the conducting shell and the plasmoid; MHD stability would thereby be provided throughout the burn without invoking active feedback stabilization. The ignited plasmoid of length ℓ enters the burn chamber with an initial velocity equal to 2-5 times ℓ/τ_s, where the electrical skin time of the stabilizing shell, τ_s, describes the decay of magnetic flux within the annular area between the first wall and the plasma separatrix. The plasmoid velocity is subsequently reduced by tailoring the flare of the shell to maintain a constant first-wall neutron loading along the full length of the burn chamber. Plasmoid motion proceeds until the velocity falls below ℓ/τ_s, at which point the reactor length is defined. The plasmoid motion terminates in an end region where expansion directly converts internal plasma energy to electrical energy. Energy confinement time scalings corresponding to classical, Alcator ($\tau_E = 3(10)^{-21} n r_p^2$) and 200 Bohm times ($\tau_E = 3.2 r_p B/T_e$) were parametrically investigated. Both Alcator and 200 Bohm confinement scalings result in plasma and overall reactor performance that is relatively insensitive to reactor length; these burns are thermally stable and eventually quench because of thermal loss after an acceptable fuel burnup and yield. As the energy confinement time is parametrically reduced, the increased plasma losses can be supplied by slightly increasing the plasma power density. This capability results in a reactor that is remarkably invariant to the assumed plasma transport as the plasmoid density and injection rate are adjustable to give a desired, axially-uniform wall loading and total power.

The plasma engineering models, system energy balances, parametric tradeoff results and the optimized design point for CTOR are given below. Although more attractive operational modes could be envisaged, this attractiveness can be gained only through added assumption at a level that is not warranted by today's knowledge of CT physics. Within the limits of the assumptions made a translating-plasmoid but steady-state reactor emerges that delivers an axially-uniform neutron wall loading of 2 MW/m^2, a net electrical power of 310 MWe from a device that is 40-m long, injects a FRC once every 5.8 s and requires a recirculating power fraction of 0.15 (engineering Q-value, $Q_E = 6.8$).

III. PLASMA ENGINEERING

A. Plasma Simulation and Energy-Balance Models

Although all results presented herein are based on dynamic zero-dimensional plasma simulations, the general tradeoffs were quantified by an analytic model[10] that was subsequently verfied by the numerical model.[12] The primary utility of the analytic model is the ability to predict plasma and system conditions where the total power output would be minimized; the analytic model could then be used to constrain numerical plasma simulations to the minimum-power condition. This minimum-power occurs for a specific value of FRC separatrix radius, r_s, and is unique to the exo-blanket conducting shell imposed on all CTOR designs. Specifically, the power output decreases as r_s is reduced as a consequence of the decreasing plasma cross-sectional area. As r_s decreases below ~ 0.8 m, however, the effective skin time required of the conducting shell, τ_s, dramatically decreases, causing the plasmoid velocity, $\sim \ell/\tau_s$, to increase; in order to meet a specific burn time, Q-value or Lawson constraint, the reactor length and total power output correspondly increases. The use of this analytic minimum-power constraint in conjunction with dynamic plasma simulations greatly facilitates the determination of the CTOR operating point. As shown in Ref. 12, this minimum-power constraint takes the form $(\Delta b + \delta/2)/r_c = 0.6(1-r_s/r_c)$. This relationship is used to select optimal design points from the large number of cases that emerge from the numerical tradeoff studies.

The plasma simulation code used to model the CTOR is based on a three-particle, time-dependent "point-plasma" model that incorporates analytical equilibrium expression,[3,10,12,13] allowing three-dimensional spatial variations to be followed in time. Starting with the post-implosion (FROP) phase, the plasma trajectory is followed through the tapered compression chamber into the burn section where conducting shell losses (translational drag) are supplied by radial plasma expansion that in turn is driven by alpha-particle heating. Referring to Fig. 1 the required radius of the conducting shell, r_c, which is positioned outside a Δb = 0.5-m thick blanket, and the plasmoid length, ℓ, are defined by experimental results ($x_s = r_s/r_c \geq 0.5$ and $\ell/r_c \geq 3.5$). In addition to the plasma burn dynamics, an overall energy balance is performed along with a spatial calculation of thermal and structural response of the first wall.

Figure 2 depicts the CTOR energy balance used to provide a measure of plant performance. A capacitor bank energy, W_{BANK}, is transferred into the FROP heating chamber with an electrical efficiency of 0.5, all losses occuring in external circuits (i.e., non-recoverable). The remaining energy forms and heats the FRC to an initial starting temperature (~ 1 keV) and provides the bias field that couples to that in the burn chamber. The FRC is then compressed to ignition using the energy from a mechanical

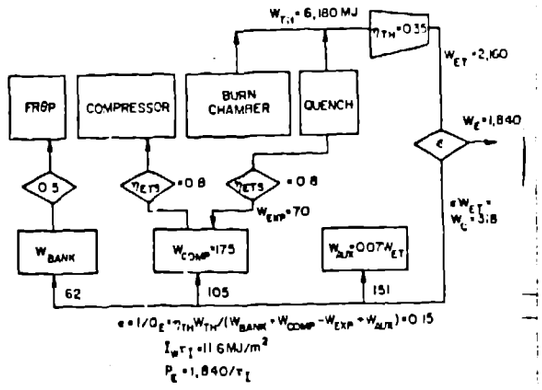

Fig. 2. Energy balance for the compact toroid reactor (CTOR).

energy store, W_{COMP}, having a transfer efficiency $\eta_{ETS} \geq 0.8$. Once again, reversible energy transfer is not assumed. Upon entering the burn chamber, translational power required to overcome resistive losses in the conducting shell would be provided directly by alpha-particle energy via plasma expansion. As the burn proceeds, plasma thermal output includes neutron, W_N, radiation, W_{RAD}, conduction, W_{COND}, and internal plasma energy W_{INT}. The plasmoid motion is terminated in a quench region where plasma expansion converts a portion (~ 30-40%) of magnetic field and internal plasma energy directly to electrical energy, W_{EXP}; this small amount of direct-conversion energy contributes to the recharge of the mechanical energy store. The remaining plasmoid energy is extracted thermally and contributes to the total thermal energy, W_{TH}, which in turn is converted to electricity with an efficiency η_{TH} = 0.35 to produce a gross electric energy, W_{ET}. Auxiliary requirements, W_A, (pumps, cryogenics, plant operation, etc.), given as a fraction f_A = 0.07 of W_{ET}, completes the energy balance. A fraction ε of the total electrical energy W_{ET} must be recirculated as makeup energy $W_C = \varepsilon W_{ET}$, the net electric energy is then $W_E = (1-\varepsilon)\, W_{ET}$, and the overall plant efficiency is $\eta_p = (1-\varepsilon)\eta_{TH}$. An engineering Q-value, Q_E, is defined below and serves as a primary object function for the system optimization

$$Q_E = W_{ET}/W_C = 1/\varepsilon$$

$$= \eta_{TH} W_{TH}/(W_{BANK} + W_{COMP} - W_{EXP} + W_{AUX}) \quad . \qquad (1)$$

Parametet studies using the plasma simulation code were performed for a range of plasmoid radii, reactor lengths, plasma densities and confinement time scalings. A plasmoid is produced by the FROP at 1.6 keV and is subsequently compressed to 8 keV in 0.1 s, requiring a radial compression factor of ~ 2.9 and an axial reduction of ~ 1.9. The ignited plasmoid enters the burn chamber with an initial plasmoid velocity equal to 2-5 times ℓ/τ_s. The velocity of the plasmoid is reduced during the translation by tailoring the flare of the burn chamber in order to maintain a constant first-wall neutron current along the burn chamber. The plasmoid velocity varies approximately as $v \propto P_\alpha/r_w$, where $P_\alpha(W)$ is the instantaneous alpha-particle power. As noted previously, motion proceeds until $v/(\ell/\tau_s) \leq 1$ at which time the translation is terminated and plasma expansion/quench occurs.

B. Parametric Studies Lending to Design-Point Determination

1. Sample Operating Point. Results from a typical burn trajectory are shown in Fig. 3 for an energy confinement equal to 200 Bohm times. This energy loss rate is extrapolated from tokamak experiments.[12] The plasmoid is assumed to lose no particles during its 1-2 s trajectory down the linear burn chamber. In effect, if the particle confinement time is on the order of τ_E, complete particle recycle with a cold gas blanket is assumed. The sample results depicted on Fig. 3 are close to the optimal design point described in Sec. IV. A thermally-stable burn results at a nearly optimal temperature of T_i = 10-14 keV, achieving a fuel burnup of $f_B \sim 0.17$ in $\tau_B = 1.96$ s for this sample case. The burn is terminated as fuel depletion, alpha-particle buildup and plasmoid expansion result in losses that ultimately overcome alpha-particle heating. The taper required of the conducting shell to overcome translational drag (Joule) losses in the stabilizing shell is shown in Fig. 3C for both an actual scale model and an exaggerated scale, the latter better illustrating radial variations. The first wall radius increases from 1.20 m to 1.64 m over a total reactor (burn section) length of 40 m for a conducting shell thickness of $\delta = 0.05$ m. Specifying the first-wall neutron loading to be uniform over the reactor length requires the plasmoid velocity to decrease from 38 m/s to 10 m/s at the outlet (Fig. 3B) where the ratio r_v, of actual velocity to minimum allowed velocity (ℓ/τ_s) is also plotted. The reactor length traversed, as defined by the trailing edge of the FRC, is also given in Fig. 3B. A comparison between the numerical solution and results from an analytic model for the case depicted in Fig. 3 is found in Ref. 12.

The results given in Fig. 3 are close to the final design point described in Sec. IV. This design point was chosen on the basis of an extensive tradeoff study utilizing the CTOR model described in Sec. III.A. The more global results of these tradeoff study are now described.

2. Parametric Tradeoff Studies. A parametric evaluation of design points for r_v = 2-5 is shown on Fig. 4 in terms of Q_E versus burn section length and various plasma densities. The thermally stable plasma burn (i.e., Fig. 3A) dictates the overall reactor length, since losses quench the burn, and translational power (i.e., alpha-particle power) is drained from the plasma to supply these transport losses. For a given plasma density the burn characteristics and Q_E are relatively insensitive to variations in L. A decrease in Q_E does occur for short reactor lengths (L = 10 m for r_{vo} = 2) because of reduced burn times and a prematurely terminated burn cycle; for long reactor length (L = 80 m for r_{vo} = 5 at $n_i = 2(10)^{21}$) increased plasmoid expansion and a lower total yield leads to a decrease in Q_E. The sample design point given in Fig. 3 occurs near the maximum Q_E value.

Also shown in Fig. 4 are dotted curves of 14-MeV neutron dose per square meter of first-wall, $I_W\tau_I(MJ/m^2)$, where $1/\tau_I$ is the FRC injection rate. A burn simulation follows the trajectory of a single plasmoid and calculates the (constant) first-wall energy density along with all other energy quantities necessary to define an overall energy balance; the first-wall loading or reactor power need not be defined until τ_I is chosen. As expected, for a given first-wall neutron loading the injection time must decrease as the length, L, increases; a larger number of FRC's are needed to supply the power in a larger device.

As shown in Ref. 12, a comparison of the numerical results with the analytic solution requires a judicious choice of r_{vo} = 3.0 to give an equivalent reactor length. Using this parameter, a spectrum of design points has been generated for Q_E versus first-wall radius (at the inlet of the burn section). These design points are shown in Fig. 5 for a range of plasma densities. Along each iso-density curve a maximum reactor length is achieved where the plasma burn optimally provides translation power. The sample design point illustrated in Fig. 3 is also shown in Fig. 5 to lie along the optimum (maximum lengths) which generally corresponds to a nearly optional (thermally stable) burn with $T_i \sim 10$-15 keV. Below this point, excessive losses lead to a low yield plasma burn with correspondingly low values of Q_E. As the first-wall radius is increased beyond that required for maximum length a thermally unstable burn drives excessive plasma length expansion; increased translational drag and correspondingly shorter systems result. A first observation indicates that this region is attractive, with shorter reactor length achievable at somewhat higher Q_E values. However, these higher Q_E values result from excessive length expansion producing more direct-conversion energy in the burn chamber and not from higher plasma yields. The physics implications of requiring large plasmoid length expansions (2-4 times starting values) for high Q_E are not resolvable. At the present level of understanding the

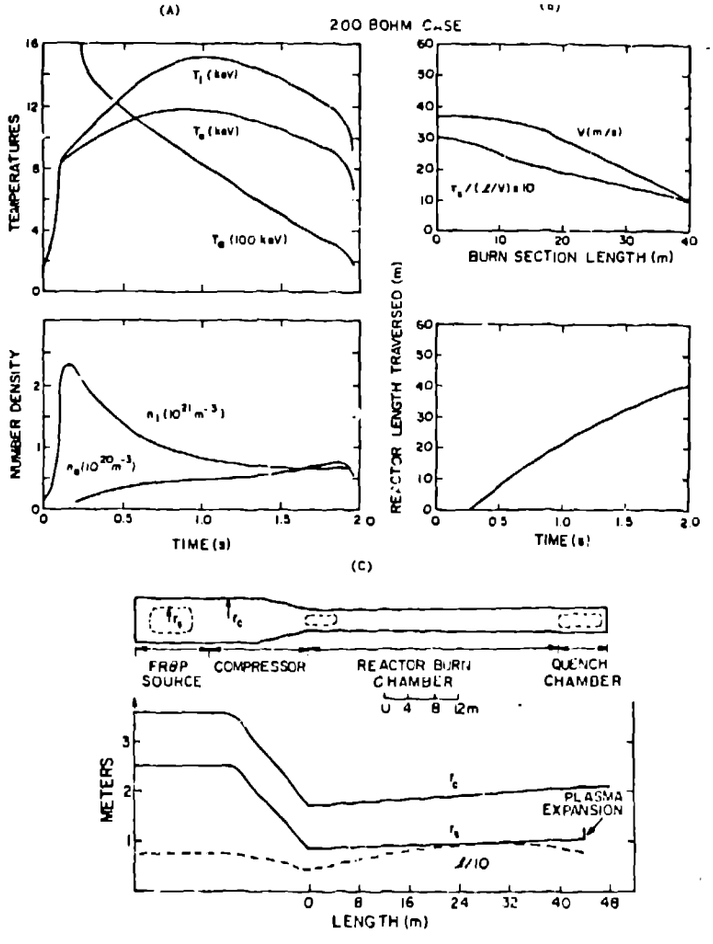

Fig. 3. Sample CTOR plasma burn.
(A) Time-dependent plasma temperatures and densities. (B) Plasmoid velocity, v, the ratio $\tau_v = v/(L/\tau_s)$ and the actual length traversed as a function of time shown. (C) Plasmoid trajectory versus reactor length showing dimensional changes in r_c, r_s and L.

thermally-stable burns are preferred and are expected to produce a more credible reactor system.

Minimizing the size of the FROP plasma source, E_s, is also desirable. Since $E_s \propto r_w^3$ for $x_s = r_s/r_c$ = constant, operation at a given Q_E for the lowest possible value of r_w is desirable. In fact, a desire to minimize the size and energy of the FROP plasmoid source is a major driving force in selecting the CTOR design point. As shown by the analytic model used to establish the minimum power condition[12], however, the total reactor thermal power increases rapidly if the radius is decreased below $r_w = 1.2$ m. A comparison between the analytic model[12] and the numerical cases (Fig. 5) for $Q_E = 7$ and $I_w = 2$ MW/m^2 is shown in Fig. 6. Using $\tau_{vo} = 3.0$ results in good agreement between the analytic and numerical results, indicating that a minimum first-wall radius of $r_w = 1.2$ m should be used for the 200 τ_{BOHM} case, as determined by the analytic model. In both the analytic and numerical cases, the burn time, τ_B, varies as $r_w^{1/2}$.

A plot of Q_E versus first-wall radius for $x_s = 0.5$ is shown in Fig. 7 for a range of Bohm scaling parameters. Increasing the loss rate requires a corresponding increase in plasma

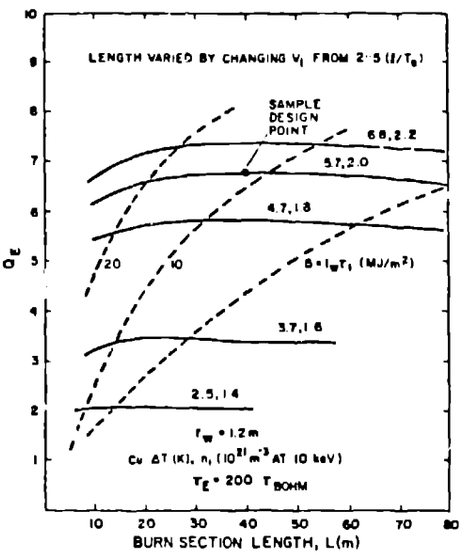

Fig. 4. A parametric evaluation of design points for r_v = 2-5 for various plasma densities. The value for ΔT is the maximum temperature drop (at burn chamber inlet) across 1 mm of water-cooled copper placed at the first wall.

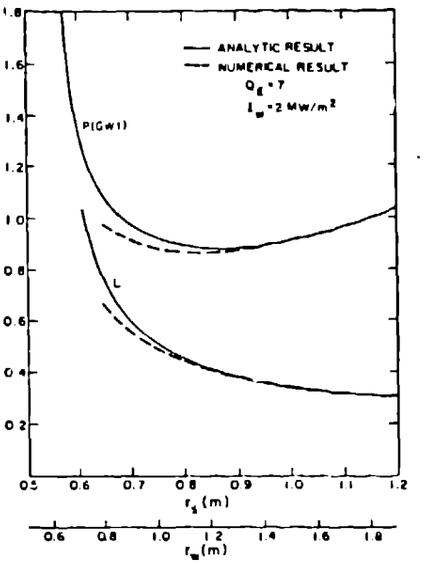

Fig. 6. Comparison of analytical and numerical predictions of P_{TH} and reactor length, L. Inlet radius, r_{wI}, is used to calculate P_{TH} in the numerical case which gives the good agreement with the analytic predictions.

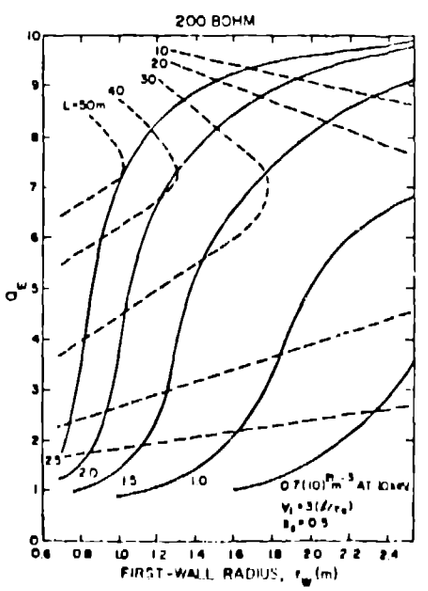

Fig. 5. Engineering Q-value, Q_E, for various plasma densities with contours of constant reactor length L.

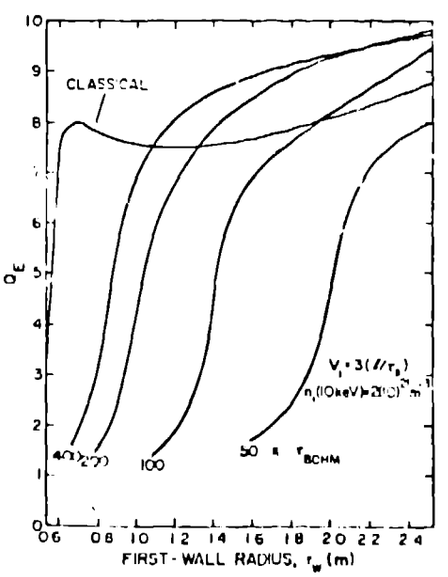

Fig. 7. Engineering Q-value, Q_E, for classical and various Bohm scalings at x_B = 0.5.

radius in order to compensate for the additional energy losses. The case where transport losses are described by classical theory results in thermal runaway and reduced yields for $r_w > 0.7$ m. Alcator scaling ($\tau_E \sim 3(10)^{21}\, na^2$), which has the same functional dependence as Bohm scaling for a high-beta plasma confined at a constant magnetic field, yielded essentially the same result as 200 Bohm.

Using the minimum-power relationships, derived from the analytic CTOR scaling,[12] the dependence of the relative thermal power and required FROP energy, E_s, is shown in Fig. 8 as a function of the Bohm multiplier. The value of r_w is taken from Fig. 7 for $Q_E = 7$ in order to generate Fig. 8 for this minimum thermal power condition. The required value of P_{TH} and E_s are normalized to 1 for the 200 Bohm design point. As shown in Ref. 12, increasing $\delta/\Delta b$ from 0.10 to 0.25 decreases P_{TH} by ~ 2, and lowering r_{vo} from 3 to 2 will further reduce the power (i.e., length) by another factor of 2 from the 1000-MWt value adopted as the design value. These reductions would lower the design-point length to only 10-m, which may not represent an economic power level.

IV. CTOR DESIGN POINT

A. Plasma and System Parameters. The sample design point discussed in Sec. III.B.1 corresponds to a 200 Bohm energy confinement time. The physics parameters for this design are listed in Table I, and the energy yields per FRC burn are given in Table II along with the system energy flows required to evaluate the engineering Q-value, Q_E. The system power is specified by choosing the injection time, τ_I. Taking $\tau_I = 5.8$ s to give a 14.1-MeV neutron wall loading of 2 MW/m^2, a thermal output of 1050 MWt results with a net electric power of 310 Mwe for $Q_E = 6.8$ and $\eta_{TH} = 0.35$. Listed in Table III are the physical parameters of the FROP, compressor section and burn section as well as key engineering parameters.

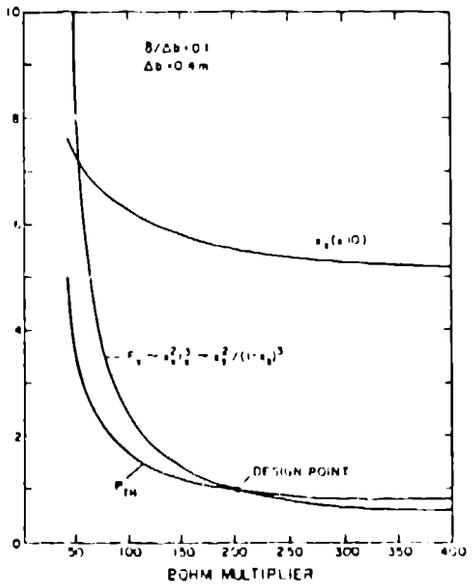

Fig. 8. Relative thermal power, P_{TH}, and plasma source (FROP) size, E_s, for various confinement times normalized to the design point value. The minimum-power constraint is imposed.[12]

B. Preliminary Plant Layout. Although the parameters given in Tables I-III are sufficiently extensive to begin a conceptual engineering design of the CTOR power plant, this aspect of the study has so far not been emphasized. Nevertheless, a preliminary plant layout has been made and is shown in Fig. 9. Future engineering studies will focus on the mechanical and electrical design of the FROP source and the compressional heater, rather than the relatively standard technology expected to be associated with the linear burn chamber.

For this 300-MWe CTOR plant, the plasma is formed in a FROP driven by a 62-MJ, 20-kV capacitor bank. The 175-MJ homopolar motor/generator powers the traveling-wave-network compressor which increases the plasma temperature from 1.5 to 8 keV at the inlet of the burn section. A 48-m long burn/quench section consists of 24 cylindrical 2-m-long modules with a solenoid superconducting coil located every 4-m (12 required). A beam dump is provided at both ends to intercept the neutron streaming with most of the alpha-particle energy retained by the plasmoid expected to exit the quench end of the device and be extracted thermally.

The burn section could be similar to the nuclear island used in the Reverse-Field Pinch Reactor.[11,14] The 0.5-m thick stainless steel blanket would contain a 40 v/o Li_2O packed bed into which penetrates radially oriented water

TABLE I

PHYSICS PARAMETERS FOR CTOR DESIGN POINT

Parameter	Value
Energy confinement time, τ_E(s)	0.1
Plasmoid translational velocity, v(m/s)	30-10
Plasma density, $n_i(10^{21}/m^3)$	2.5-0.5
Plasma temperature, T_i(keV)	~ 15
Ion-gyroradii in column, R/ρ_{i0}	170
Ion-gyroradii to minor radius, $S = a/\rho_i$	30.
Beta, $\beta_s = 1 - 0.$ [illegible]^2	0.87
Separatrix ratio, $x_s = r_s/r_c$	0.5
Burn time, τ_b(s)	1.95
Burnup, f_B	0.17
Lawson parameter, $n\tau_B(10^{20}$ s/m$^3)$	21.0

TABLE II

ENERGY INVENTORY FOR CTOR DESIGN POINT[a]

Parameter	Value (MJ/FRC)
Initial plasma	16.4
Final plasma	81.7
Neutron (16.5 MeV/n)	5090.
Alpha particle	1090.
Direct conversion	32.6
Bremsstrahlung	9.1
Thermal conduction	897.
Trapped poloidal flux (quench)	7.0
Quench	88.8
Total thermal	6170.
Conducting shell transport losses[b]	46.3
Auxiliary, W_{AUX}	151.
ETS losses (η_{ETS} = 0.8), W_{ETS}	80.
FROP source bank, W_{BANK}	61.8
Homopolar compressor, W_{COMP}	175.
Homopolar recharge at quench, W_{EXP}	70.
Gross electric (η_{TH} = 0.35)	2160.
Circulating electric	318.
Net electric	1840.

[a] Refer to CTOR energy balance, Fig. 2.
[b] provided by alpha-particles expansion of the FRC plasmoid

steam cooled U-tubes. A low-pressure (0.1 MPa) helium purge gas is drifted through the granular Li_2O bed to extract tritium as an oxide. The slightly superheated (5-K) steam emerging from this blanket would be used to drive a turbo-generator. Despite the pulsed (plasma) nature of the burn, the inherent thermal capacity of this blanket results in less than a 5-K temperature excursion within the blanket structure, although a 1.0-mm-thick copper first-wall undergoes a bulk rise of 26 K (ΔT = 6 K across the material, leading to thermal stresses of 1.2 MPa at the inlet end of the burn chamber). A shield composed of a 0.1-m thick lead and a 1.4-m thick borated-water region protects the relatively low field (1.5-3.0 T) NbTi-Cu superconducting magnet coils (15 MA/m^2 average current density exclusive of support structure) from thermal loading and neutron/gamma-ray damage. Each of the 2-m long burn section modules would be electrically and thermohydraulically independent. The solenoidal field coils would be fixed structures that are adequately spaced to permit removal of the shield and blanket modules. The magnet coils and shield modules are of equal dimensions along the length of the burn section, while the elements of the first wall and blanket are made progressively larger (in a step-wise fashion) along the axial length to provide the modest taper required for alpha-particle-driven plasmoid expansion and translation.

TABLE III

CTOR ENGINEERING PARAMETERS

FROP Plasma Source	Value
Number of coils	2
Radius (m)	3.4
Length (m)	5 (each)
Capacitor energy, W_{BANK} (MJ)	62
Terminal voltage, V_0 (kV)	20
Electric field, E_0 (kV/cm)	0.95
Risetime, τ_R (μs)	47.
Pre-implosion pressure, P_A (mTorr)	0.5
Post-implosion density, $n_o(10^{20}/m^3)$	1.4
Compressor	
Radius (tapered), r_c(m)	3.4-1.7
Length (m)	16
Homopolar specifications	
• Energy (MJ)	175
• Efficiency	0.8
• Risetime (s)	0.1
Peak voltage (kV)	5
Peak current (MA)	0.7
Burn Section	
Length, L(m)	40
Tapered first-wall radius, r_w(m)	1.2-1.6
Blanket thickness, Δb(m)	0.48
Conducting shell	
• Thickness (m)	0.05
• Fraction of conductor in shell	0.7
Shield thickness (m)	1.5
Superconducting coil	
• Radius (m)	3.2-3.6
• Magnet field (T)	3.1-1.5
Maximum first-wall thermal response[a]	
• Bulk temperature rise (K)	23
• Thermal differential, (K)	6
• Thermal stress (MPa)	1.2
Overall Reactor Performance	
Engineering Q-value, Q_E	6.8
Recirculating power fraction, ϵ	0.15
First-wall loading, l_W (MW/m^2)	2.0
Injection time, τ_I(s)	5.8
Total thermal power, P_{TH} (MWt)	1050
Gross electric, P_{ET} (MWe)	365
Recirculating power, P_c (MWe)	55
Net electric power, P_E (MWe)	310
Thermal conversion efficiency, η_{TH}	0.35
Plant efficiency, $\eta_p = \eta_{TH}(1-\epsilon)$	0.30

[a] excursion in 1.0-mm-thick water-cooled copper at most severe location (burn chamber inlet).

Maintenance equipment for this system is also indicated in Fig. 9. The entire CTOR is located inside a vacuum tunnel which allows

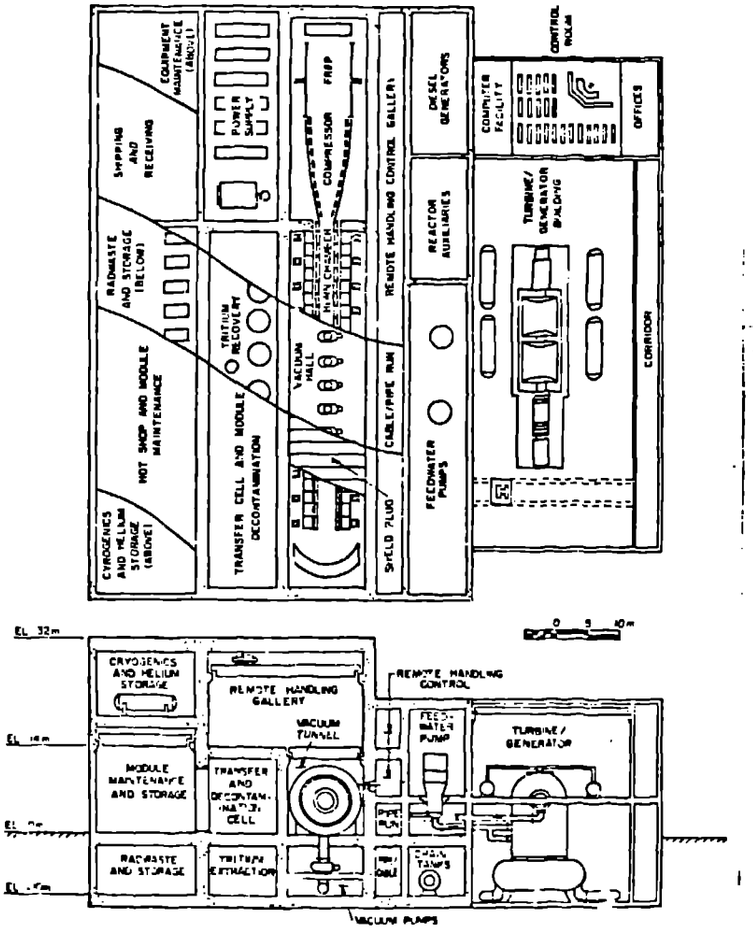

Fig. 9. Preliminary plant layout.

relatively easy access to the vacuum seals (shield plugs). Upon removal of three adjacent 2-m-long shield plugs, two solenoidal magnet coils are uncovered. The top-hemicylindrical half of the water shield would be removed between the fixed superconducting coils. Simple translating motions then allow the other two shield sections (located under the magnet coils) to be removed, uncovering three 2-m long first-wall/blanket modules. These modules are transferred to the adjacent decontamination cell and ultimately are moved into the hot cell facility.

V. CONCLUSIONS AND FUTURE DIRECTIONS

A parametric evaluation of sample design points for a Compact Toroid reactor that uses Field-Reversed Theta Pinch for a plasma source has been performed numerically for a wide range of plasma transport, plasma densities, reactor radii and lengths. For an energy confinement time of 200 Bohm times (projected from tokamak confinement) an optimal burn is achieved at a first-wall radius of 1.2 m. The radius of the conducting shell must be tapered 40% (1.7 m to 2.1 m) over the 40-m reactor length as the plasmoid velocity varies from 30 to 10 m/s. The reactor length could be shortened by increasing the shell thickness ($\delta \sim 0.05$ m) or decreasing the inlet plasmoid velocity; the 40-m reactor length is considered to give an optimal system, however, in terms of minimizing the FROP source requirements simultaneously with minimizing the total reactor power output. This reactor produces 310 MWe with a recirculating power fraction of 0.15. Smaller radius systems are achievable, although to maintain a good energy balance, the plasma density must be increased, leading to a higher first-wall thermal cycle.

Generally, the CTOR is represented as a high-Q system of modest size. The pulsed energy storage requirements are only ~ 60 MJ of capacitive energy for the FROP and a 175-MJ homo-

polar generator. Energy recovery is achieved in the quench region without the use of opening switches, with the plasma motion providing the necessary switching characteristics. The high-voltage and active source elements have been completely removed from the totally passive burn section. The linear system configuration simplifies maintenance and construction procedures. A natural divertor is also presented by the open-field line geometry outside the separatrix.

The realization of this attractive system is contingent upon the transport properties assumed for the plasma. Systems with high losses ($\tau_E \sim$ 0.1 s for the design plant) will either require higher operating densities (leading to higher first-wall thermal cycle) or systems of larger radial dimensions. Since the size of the source requirements increase as $\sim nr_w^3$, larger pulsed power requirements are imposed. Particle transport may also have adverse effects on the burn cycle. The batch burn system used here assumes little change in the particle inventory, during the $\sim$ 2-s burn. Particle loss is likely to occur along with injestion of gas streaming to the plasmoid from the quench region. The competition of these two processes will determine the time-dependent particle inventory, a process that requires more detailed modeling.

Recommendations for future work include primarily engineering considerations, although further understanding of plasma transport must be incorporated in the design-point determination. Detailed designs of the FROP and compressor sections must be undertaken to define more clearly the energy losses and physical dimensions of these two important systems. Slower plasma sources, such as the coaxial theta-pinch, should be investigated in order to minimize the use of high-voltage elements. The quench region must also be more clearly defined along with the necessary neutral particle densities needed to quench the plasma. Implications of the power streaming from the plasma and deposited at reactor ends requires quantification; such streaming is expected to result in a density gradient along the machine which will certainly impact energy/particle transport. The first-wall/blanket temperature and mechanical stresses must be optimized in terms of burn chamber lifetime and required maintenance intervals; even more conventional thermal systems, such as the pressurized water blanket system proposed for the Starfire tokamak reactor,[15] should be considered. Maintenance procedures and overall plant layout would also be refined. Lastly, a technological assessment of the CTOR plant should then be made particularly with respect to the new technologies required of the plasma source, heater and quench sections.

REFERENCES

1. H. Alfven, "Magnetohydrodynamics and the Thermonuclear Problem," 2nd UN Conf. on the Peaceful Uses of Atomic Energy, 31, 3-5 (1958).

2. M. N. Bussac, H. P. Furth, M. Okabayashi, M. N. Rosenbluth, and A. M. M. Todd, "Low-Aspect-Ratio Limit of the Toroidal Reactor: The Spheromak," Proc. of the 7th Inter. Conf. on Plasma Physics and Controlled Nuclear Fusion Research IAEA-CN-37/X-1, III, 249-264 (1978).

3. H. Furth, "The Compact Torus Concept and the Spheromak," Proc. US/Japan Joint Symp. on Compact Toruses and Energetic Particle Injection, Princeton Plasma Physics Laboratory, Princeton, NJ, 3-7 (December 12-14, 1979).

4. G. A. Carlson, W. C. Condit, R. S. Devoto, J. H. Fink, J. D. Hanson, W. E. Neef, and A. C. Smith, Jr., "Conceptual Design of the Field-Reversed Mirror Reactor," Lawrence Livermore Laboratory report UCRL-52467 (1978).

5. A. C. Smith, Jr., G. A. Carlson, K. R. Schultz, W. S. Neef, D. M. Woodall and R. E. Price, "Preliminary Conceptual Design of the Moving Ring Field-Reversed Mirror Reactor," Pacific Gas and Electric Company report 78FUS-1 (1978).

5A. C. H. Choi, J. G. Gillegan and G. H. Miley, "The Saffire D-3 He Pilot Plant Concept," 1979 Annual report Fusion Studies Laboratory, University of Illinois.

6. A. M. M. Todd, R. E. Olson, J. G. Gilligan and G. H. Miley, "The Spheromak Fusion Reactor," Proc. 15th Intersoc. Energy Conversion Eng. Conf., 3, 2229-2236 (August 18-22, 1980).

7. R. L. Miller and R. A. Krakowski, "Reassessment of the Slowly-Imploding Liner (LINUS) Fusion Reactor Concept," Los Alamos Scientific Laboratory report (to be published, 1980).

8. H. J. Willenberg, L. C. Steinhauer, A. L. Hoffman, T. L. Churchill, and P. H. Rose, "TRACT: A Small Fusion Reactor Based on Near-Term Engineering," Proc. 15th Intersoc. Energy Conversion Eng. Conf. 3, 2214-2220 (August 18-21, 1980).

9. H. H. Fleischmann and T. Kammash, "System Analysis of the Ion-Ring Compressor Approach to Fusion," Nucl. Fus., 15, 1143-1155 (1975).

10. R. L. Hagenson and R. A. Krakowski, "Conceptual Physics Design of a Compact Torus Fusion Reactor (CTOR)," Los Alamos Scientific Laboratory report LA-8448-MS (July, 1980).

11. R. Hancox, R. A. Krakowski, W. R. Spears and R. L. Hagenson, "The Reverse-Field Pinch Reactor," Nucl. Eng. and Design (to be published, 1980).

12. R. L. Hagenson and R. A. Krakowski, "Design-point Determination for the Compact Torus Reactor (CTOR)," Los Alamos Scientific Laboratory report to be published (1980).

13. W. T. Armstrong, S. K. Linford, J. Lipson, D. A. Platts and E. G. Sherwood, "Field Reversed Experiments (FRX) on Compact Toroids," submitted to Physics of Fluids (1980).

14. R. L. Hagenson, R. A. Krakowski and G. E. Gort, "The Reversed-Field Pinch Reactor (REPR) Concept," Los Alamos Scientific Laboratory report LA-7973-MS (August, 1979).

15. C. C. Baker, G. A. Carlson and R. A. Krakowski, "Trends and Developments in Magnetic Confinement Fusion Reactor Concepts," Nuclear Technology - Fusion (to be published, 1981).